

SUPPLEMENTARY MATERIAL TO  
**Chemical reactivity of alliin and its molecular interactions with  
the protease M<sup>pro</sup> of SARS-CoV-2**

WENDOLYNE LÓPEZ-OROZCO, LUIS HUMBERTO MENDOZA-HUIZAR\*, GIAAN  
ARTURO ÁLVAREZ-ROMERO, JESÚS MARTÍN TORRES-VALENCIA  
and MARICRUZ SANCHEZ-ZAVALA

*Academic Area of Chemistry, Universidad Autónoma del Estado de Hidalgo, Carretera  
Pachuca-Tulancingo, 42184, Mineral de la Reforma, Hidalgo, Mexico*

*J. Serb. Chem. Soc.* 89 (11) (2024) 1433–1445

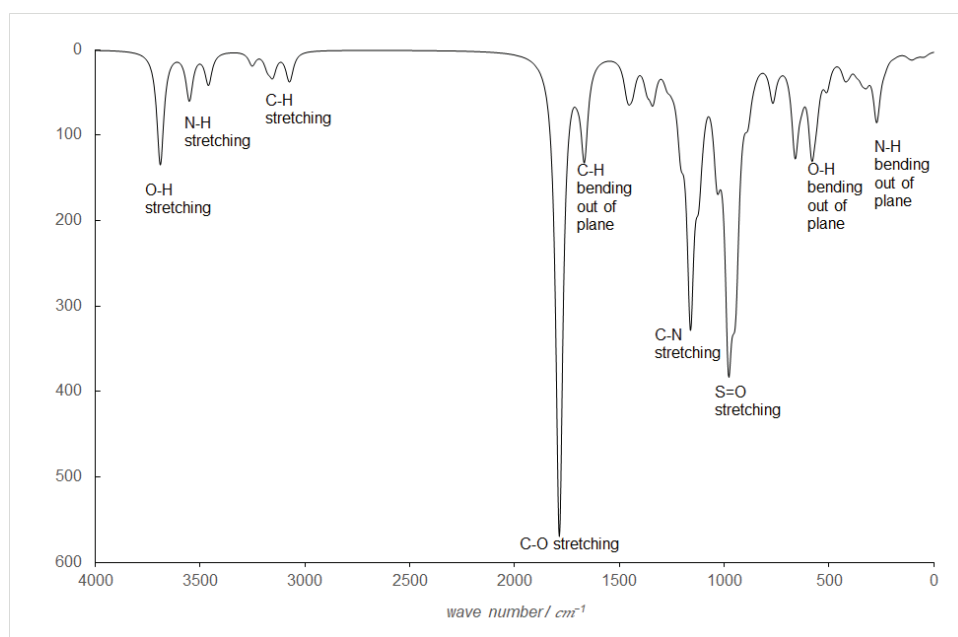


Figure S-1: Theoretical IR spectra of alliin in the aqueous phase obtained at the B3LYP/DGDZVP level of theory.

\* Corresponding author. E-mail: hhuizar@uaeh.edu.mx

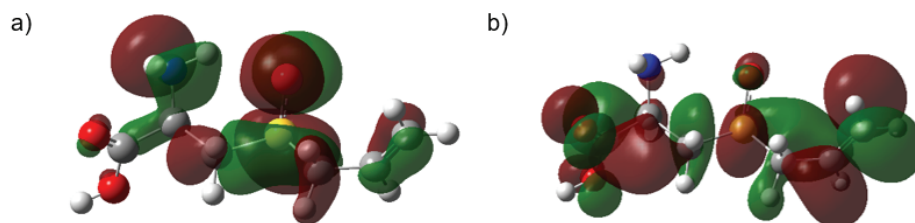


Figure S-2. HOMO and LUMO distributions on alliin obtained at the B3LYP/DGDZVP level of theory in the gas phase. In all cases the isosurfaces were obtained at  $0.08 \text{ e/u.a.}^3$ .

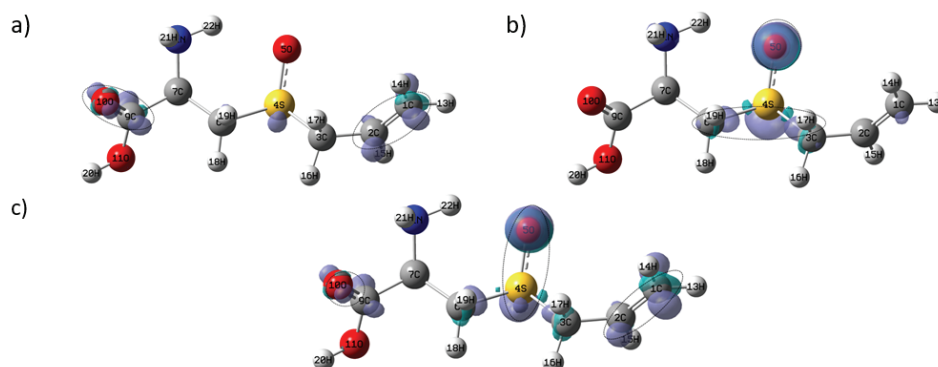


Figure S-3. Isosurfaces of Fukui Functions for alliin according to equations (9), (10) and (11) at the B3LYP/DGDZVP level of theory in the gas phase. In the case of (a) nucleophilic, (b) electrophilic and (c) free radical attacks. In all cases the isosurfaces were obtained at  $0.008 \text{ e/u.a.}^3$ . The dotted circles show the most reactive zones in each molecule.

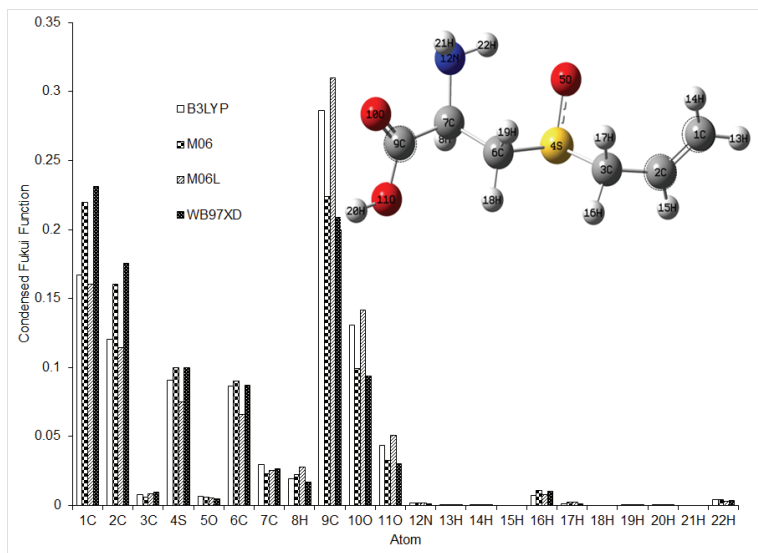


Figure S-4. Condensed Fukui function values for electrophilic attacks on alliin at the X/DGDZVP level of theory (where X=B3LYP, M06, M06L and  $\omega$ B97XD), in the aqueous phase employing the Hirshfeld population and equations (12)-(14), the dashed circles show the most reactive zones in each molecule.

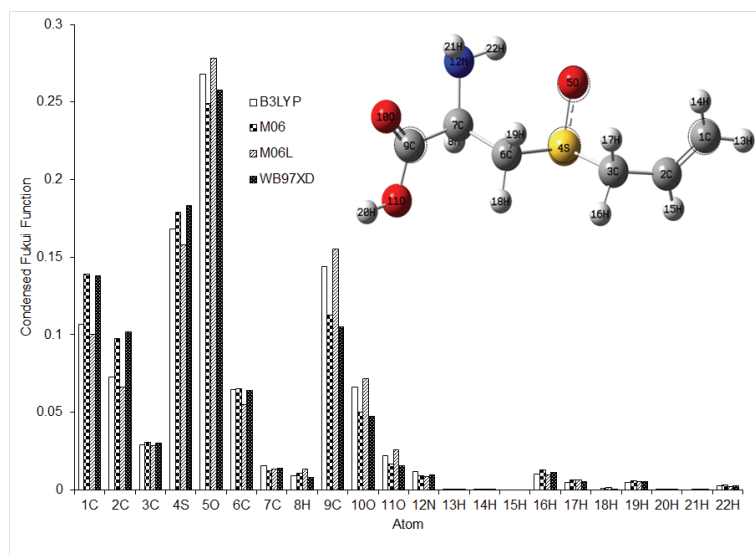


Figure S-5. Condensed Fukui function values for free radical attacks on alliin at the X/DGDZVP level of theory (where X=B3LYP, M06, M06L and  $\omega$ B97XD), in the aqueous phase employing the Hirshfeld population and equations (12)-(14), the dashed circles show the most reactive zones in each molecule.

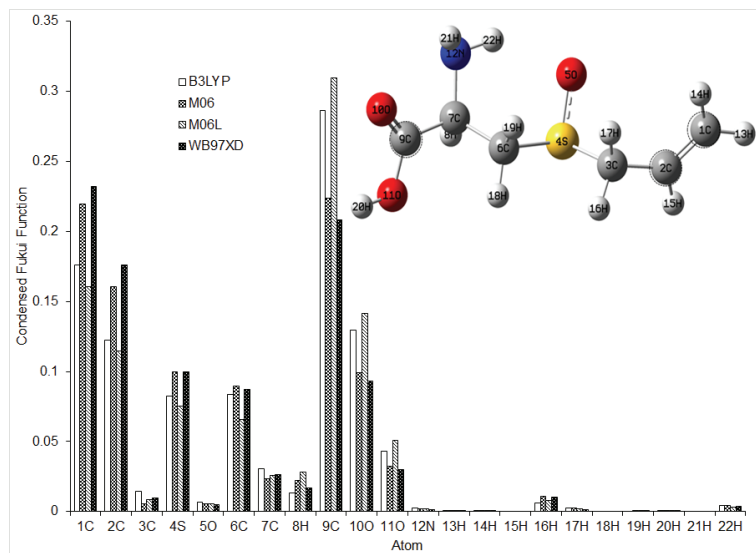


Figure S-6. Condensed Fukui function values for nucleophilic attacks on alliin at the X/DGDZVP level of theory (where X=B3LYP, M06, M06L and  $\omega$ B97XD), in the gas phase employing the Hirshfeld population and equations (12)-(14), the dashed circles show the most reactive zones in each molecule.

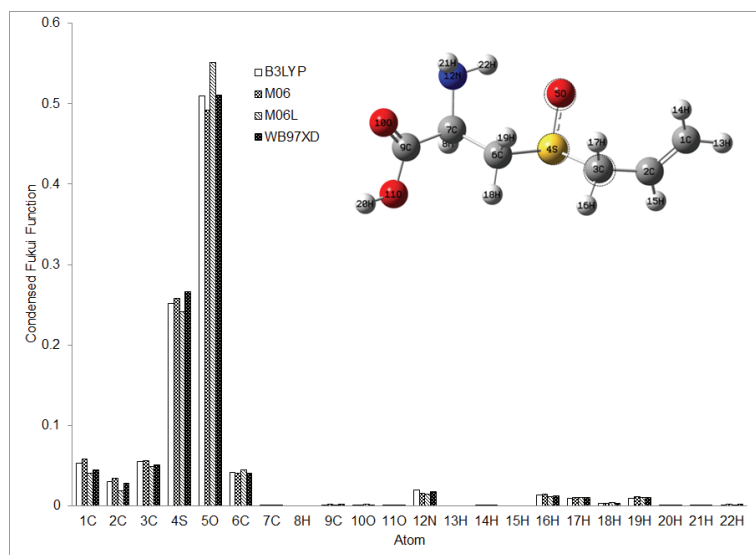


Figure S-7. Condensed Fukui function values for electrophilic attacks on alliin at the X/DGDZVP level of theory (where X=B3LYP, M06, M06L and  $\omega$ B97XD), in the gas phase employing the Hirshfeld population and equations (12)-(14), the dashed circles show the most reactive zones in each molecule.

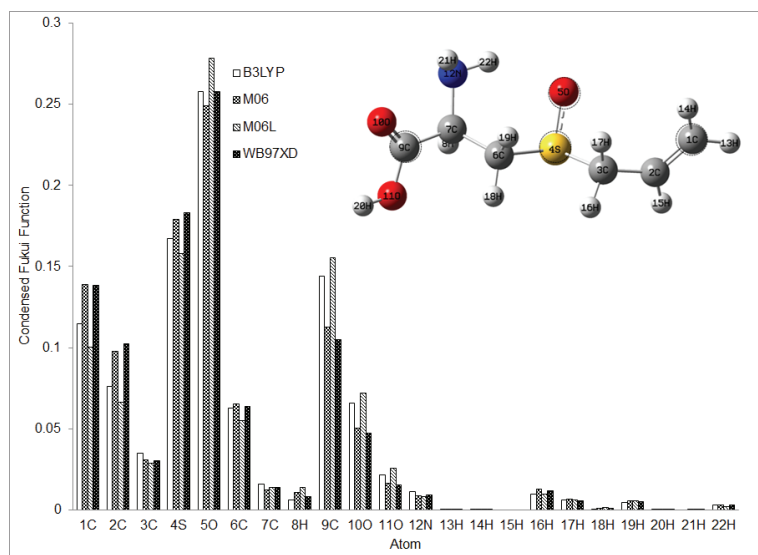


Figure S-8. Condensed Fukui function values for free radical attacks on alliin at the X/DGDZVP level of theory (where X=B3LYP, M06, M06L and  $\omega$ B97XD), in the gas phase employing the Hirshfeld population and equations (12)-(14), the dashed circles show the most reactive zones in each molecule.

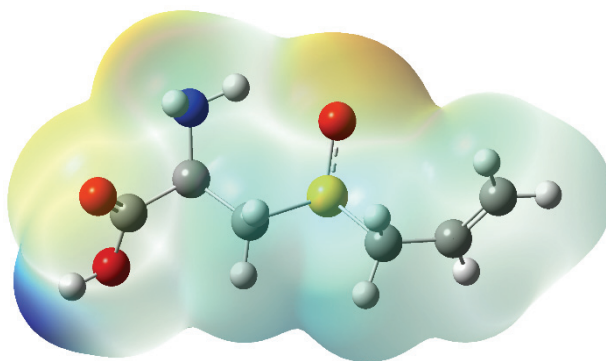


Figure S-9. Mapping of electrostatic potentials evaluated at the B3LYP/DGDZVP level of theory in the gas phase, over a density isosurface (value =  $0.002 \text{ e/a.u.}^3$ ) for alliin.

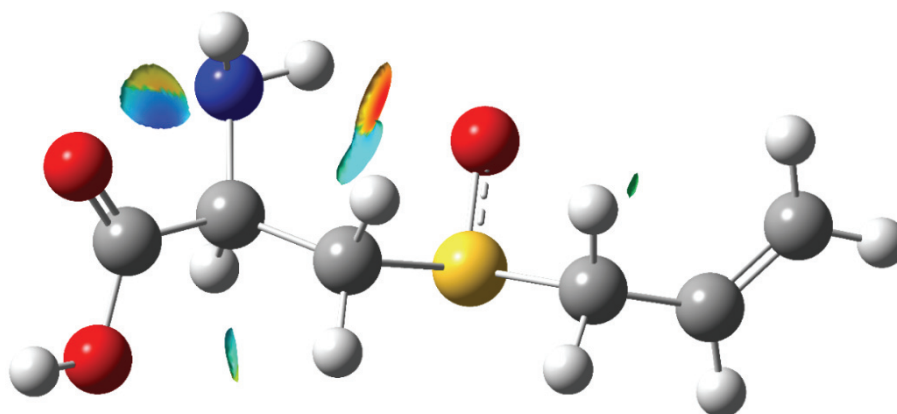


Figure S-10. Isosurface area of NCI = 0.2 for alliin in aqueous phase.

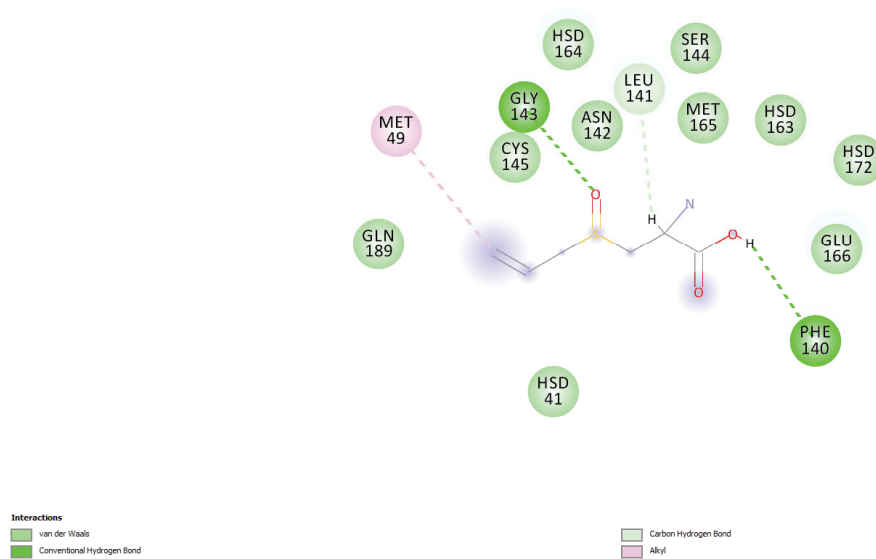


Figure S-11. 2D mapping of ligand/protein interactions for alliin.